Title	Efficient condensation of organic colloids in deep groundwater using surface-modified nanofiltration membranes under optimized hydrodynamic conditions
Author(s)	Aosai Daisuke, Saeki Daisuke, Iwatsuki Teruki, Matsuyama Hideto
Citation	Colloids and Surfaces A; Physicochemical and Engineering Aspects, 495, p.68-78
Text Version	Author's Post-print
URL	https://jopss.jaea.go.jp/search/servlet/search?5055024
DOI	https://doi.org/10.1016/j.colsurfa.2016.01.057
Right	© 2016. This manuscript version is made available under the CC-BY-NC-ND 4.0 license http://creativecommons.org/licenses/by-nc-nd/4.0/

Submitted to Colloids and Surfaces A, 2015

Efficient condensation of organic colloids in deep groundwater using surface-modified nanofiltration membranes under optimized hydrodynamic conditions

Daisuke Aosai[a], Daisuke Saeki[a], Teruki Iwatsuki[b], Hideto Matsuyama[a,*]

[a] Center for Membrane and Film Technology, Department of Chemical Science and Engineering, Kobe University, 1-1 Rokkodai, Nada, Kobe 657-8501, Japan

[b] Japan Atomic Energy Agency, 1-64 Yamanouchi Akeyo, Mizunami, 509-6132, Japan

*Corresponding author.

E-mail address: matuyama@kobe-u.ac.jp (H. Matsuyama).

Abstract

The transport of radionuclides by organic colloids in deep groundwater is one of the important issues for the geological disposal of high-level radioactive waste. Because of their low concentration, it is difficult to directly analyze organic colloids in deep groundwater. Hence, it is useful to utilize porous membranes for the condensation which can increase the concentration of organic colloids in groundwater physically without alteration of their properties, although some part of the components is lost by membrane fouling. In this study, hydrodynamic conditions were optimized, and surfaces of nanofiltration (NF) membranes were modified using a cationic phosphorylcholine polymer, poly(2-methacryloyloxyethyl phosphorylcholine-co-2-aminoethyl methacrylate) (p(MPC-co-AEMA)), for preventing membrane fouling and improving condensation efficiency. Aqueous solutions of humic acid or bovine serum albumin (BSA) were used as models of organic colloids, and they were condensed using a laboratory-scale cross-flow filtration apparatus equipped with a commercial sulfonated polyethersulfone NF membrane. The effects of hydrodynamic conditions, such as the applied transmembrane pressure (TMP) and stirring rate, and membrane surface modification on condensation efficiency were evaluated. A low TMP and high stirring rate effectively improved the recovery yield of humic acids and BSA. The membrane surface coated with p(MPC-co-AEMA) was significantly effective for preventing the decline in permeate flux, caused by fouling with BSA. Deep groundwater, obtained from a depth of 300 m at the Mizunami Underground Research Laboratory in Japan, was condensed. The recovery yield of the organic colloids in the deep groundwater condensation test at 5-fold condensation was improved from 62% to 92% by the optimized hydrodynamic conditions and membrane surface modification for prevention of membrane fouling. The composition of organic colloids in the condensates was analyzed using pyrolysis gas chromatography coupled with mass

spectrometry.

Keywords: Condensation, Nanofiltration membrane, Organic colloid, Groundwater, Hydrodynamic condition, Membrane surface modification

1. Introduction

High-level radioactive waste (HLW) originating from the nuclear industry is legislated to be disposed of underground at a depth of more than 300 m [1]. The safety of the geological disposal of HLW is dependent on the migration of the radionuclides released from HLW into the underground environment. Organic colloids are present in deep groundwater [2,3], and the interaction between organic colloids and radionuclides affects the migration of radionuclides [4,5]. Therefore, for the safety assessment of HLW, it is imperative to understand the detailed composition of organic colloids and their interaction with radionuclides. Precise analysis of organic colloids from groundwater is difficult, caused by their low concentration [6,7]; hence, extraction techniques using adsorption resins [8,9] are widely applied. However, extracted samples using adsorption resins are exposed to severe chemical disturbances, and there is concern over their chemical changes. On the other hand, condensation using porous membranes has also been applied to afford high concentrations of organic colloids. Although porous membranes can rapidly condense organic colloids without chemical exposure [10–12], some amount of organic colloids from the condensed samples is lost because of their deposition on the membrane surface and subsequent blocking of pores (membrane fouling). For obtaining more accurate information on organic colloids, it is imperative to prevent membrane fouling.

Effects of hydrodynamic conditions on membrane fouling by organic colloids have been investigated [13–15]. These studies have reported that membrane fouling is affected by chemical and hydrodynamic interactions. That is, the fouling of membranes by organic colloids is promoted by high concentrations of divalent cations (Ca^{2+} and Mg^{2+}), high initial permeate flux, and low cross-flow velocity. Divalent cations neutralize the net negative charge of humic acids, which supposedly constitute the majority of organic colloids in groundwater, resulting in the

reduction of repulsion among humic acid molecules [16–18]. In addition, divalent cations can bridge humic acid molecules [19]. Thus, divalent cations accelerate the fouling of membranes, caused by the coagulation of humic acid molecules. The high permeate flux or low cross-flow velocity increases the concentration of divalent cations on the membrane surface, caused by concentration polarization, which in turn enhances membrane fouling [14]. Thus, increase in the cross-flow velocity and decrease in the permeate flux mitigate the fouling of membranes by organic colloids.

The surface modification of membranes using various hydrophilic polymers has also been effective for preventing membrane fouling [20]. Hydrophilic polymers, such as polyethylene glycol, and zwitterionic polymers have been frequently used for modifying the surfaces of porous membranes with the aim of preventing the adsorption of organic colloids and fouling of membranes [21–24]. We have developed a simple, facile method for modifying polyamide reverse osmosis (RO) membranes using zwitterionic polymers with the aim of preventing the adsorption of bacteria [25]. Negatively charged RO membranes were coated with poly(2-methacryloyloxyethyl phosphorylcholine-co-2-aminoethyl methacrylate) (p(MPC-co-AEMA)), which is composed of cationic AEMA units and zwitterionic MPC units, by electrostatic interaction. The coated RO membranes exhibited high hydrophilicity and high resistance to bacterial adsorption. Therefore, membrane surface modification with p(MPC-co-AEMA) is also promising for preventing the fouling of membranes by organic colloids.

Previously, we have developed a method for the condensation of organic colloids in groundwater using nanofiltration (NF) membranes [12]. The use of NF membranes facilitated the condensation of organic colloids without severe reduction in flux, while condensation using RO

membranes facilitated severe reduction in flux, caused by the precipitation of condensed inorganic substances. Organic colloids in actual condensed groundwater at a depth of 300 m in granitic rocks were successfully analyzed by pyrolysis gas chromatography coupled with mass spectrometry (Py-GC/MS), and their composition was similar to that of humic substances with high humification. However, the recovery yields of organic colloids were up to 57% at 20-fold condensation, caused by the fouling of organic colloids. Thus, the recovery yields need to be improved for the purpose of confirming the validity of the result obtained by Py-GC/MS.

This study aimed at preventing the fouling of membranes by organic colloids in the condensation of deep groundwater using NF membranes by optimizing hydrodynamic conditions and modifying the membrane surface. Commercial humic acids and bovine serum albumin (BSA) were used as models of organic colloids. The aqueous solutions of organic colloids were condensed using a cross-flow filtration apparatus equipped with sulfonated polyethersulfone NF membranes. The time courses of permeate flux and the recovery yield of humic acid and BSA were monitored. The effects of hydrodynamic conditions and membrane surface modification with p(MPC-co-AEMA) on condensation behavior were examined. Finally, actual deep groundwater was condensed using modified NF membranes under optimized hydrodynamic conditions. The composition of the organic colloids in the condensed deep groundwater was analyzed by Py-GC/MS.

2. Experimental

2.1. Materials

All solutions used in this study were prepared using ultrapure water and analytical-grade chemicals. Unless specified, all chemicals were obtained from Wako Pure Chemical Industries

(Osaka, Japan) and were used without further purification. Commercial sulfonated polyethersulfone NF membranes were obtained from Nitto Denko (NTR7450; Osaka, Japan). Coal-derived humic acid (WHA; 088-04622; Wako Pure Chemical Industries) and peat-derived humic acid (AHA; H16752; Sigma-Aldrich, St. Louis, MO, USA) were used after purification according to a previous study [12]. A p(MPC-co-AEMA) (MPC:AEMA = 9:1, random copolymer) was generously supplied by NOF Corporation (Tokyo, Japan), and its weight-average molecular weight was 9.7×10^5 [25]. Coomassie brilliant blue (CBB) G-250 was purchased from Polysciences Inc. (Warrington, PA, USA).

Groundwater in the granitic rock was collected from the 09MI20 borehole in the −300 m Access/Research Gallery of Mizunami Underground Research Laboratory on December 25, 2014. The borehole was divided into six sections by impermeable packers, and the sections were numbered from 1 to 6 according to the distance from the base of the borehole. Groundwater samples were collected from section 1 and placed in the refrigerator until experiments were conducted. Detailed information of the borehole and hydrochemistry of the examined groundwater has been summarized in our previous paper [12]. The groundwater contained 9.0 mg/L Ca^{2+}, and the pH was 8.5.

2.2. Condensation apparatus

Fig. 1 shows the laboratory-scale cross-flow membrane filtration apparatus used for condensation experiments [12]. For condensation experiments, a feed solution was fed into a cylindrical stainless steel membrane cell using a plunger pump (NPL-120; Nihon Seimitsu Kagaku, Tokyo, Japan) at a constant flow rate of 9.0 mL/min. The applied transmembrane pressure (TMP) was adjusted at 0.75 MPa or 1.5 MPa using a back pressure valve. The effective

membrane area was 8.0 cm^2. The permeate solution was collected in a permeate reservoir. The retentate solution was circulated through the feed reservoir and was condensed. The feed solution in the cell was stirred using a cylindrical magnetic bar with a length of 3.0 cm at 150 or 1500 rpm. Permeate flux was calculated from the time course of permeate weight.

2.3. Modification of membrane surface using a cationic phosphorylcholine polymer

A negatively charged NF membrane was modified using cationic p(MPC-co-AEMA) by electrostatic interaction [25]. As shown in Fig. 1, the NF membrane was set into the membrane cell. An aqueous solution of 0.1 wt% p(MPC-co-AEMA) was fed into the membrane cell at a constant flow rate of 9.0 mL/min and a constant TMP of 0.75 MPa for 2 h. The feed solution of the membrane cell was magnetically stirred at 150 rpm. Then, the membrane was detached and washed by gentle shaking in an aqueous solution of 3.5 wt% NaCl for removing non-specifically adsorbed polymers. For evaluating the surface hydrophilicity of the membranes, the water contact angle was measured using a contact angle meter (DM-300; Kyowa Interface Science, Saitama, Japan). The ζ-potential was measured by streaming potential measurement using an electrophoretic light-scattering apparatus (ELSZ-1000, Otsuka Electronics, Osaka, Japan) in aqueous 10 mmol/L NaCl.

2.4. Condensation of humic acid and BSA

A feed solution of 5 mg/L of humic acid containing 1 mg/L Ca^{2+} or 5 mg/L of BSA was condensed from 125 mL to 25 mL (5-fold condensation) using the raw NF membrane and p(MPC-co-AEMA)-coated NF membrane under different TMPs (0.75 or 1.5 MPa) and stirring rates (150 or 1500 rpm). The concentration of Ca^{2+} in the feed solution of humic acid was

156 adjusted using a 1000 mg/L Ca^{2+} standard solution composed of $CaCO_3$ in 0.1 mol/L HNO_3
157 (Wako Pure Chemicals).

158 The humic acid concentration was determined by optical density measurements at 254 nm
159 using a UV–vis spectrometer (V-650; Jasco Corp., Tokyo, Japan). The BSA concentration was
160 determined by a CBB method [26]. CBB was dissolved in methanol, and then phosphoric acid
161 and ultrapure water were added. The final concentration of the components in this CBB solution
162 was 0.025% (w/v) CBB, 12.5% (w/v) methanol, and 70.83% (w/v) phosphoric acid. The CBB
163 solution (0.2 mL) and 0.8 mL of the sample were mixed, and the optical density at 595 nm was
164 measured using a UV–vis spectrometer. To evaluate condensation efficiency, the recovery yield
165 was defined as the amount of humic acid or BSA in the condensed solution divided by that in the
166 initial solution.

167

168 *2.5. Characterization of organic colloids*

169 Condensation experiments were carried out using groundwater. The concentration of organic
170 colloids in the groundwater was determined by the same method as that used for the
171 determination of humic acid under the assumption that all organic colloids are humic acids. The
172 condensed organic colloids were characterized by Py-GC/MS. Py-GC/MS analysis was carried
173 out using a double-shot pyrolyzer (PY-2020id; Frontier Laboratories Ltd., Fukushima, Japan)
174 attached to a GC/MS instrument (Agilent 6890N/Agilent 5973; Agilent Technologies Inc., Palo
175 Alto, CA, USA) Py-GC/MS is a powerful tool for obtaining detailed compositional information
176 of a polymer. Two humic acids derived from coal and peat were directly analyzed by Py-GC/MS.
177 In the case of the organic colloids in condensed groundwater, the condensed water was further
178 evaporated, dried under N_2, and then analyzed by Py-GC/MS. Py-GC/MS analysis was

179 performed by the same method as in our previous paper [12].

180

181 **3. Results and discussion**

182 *3.1. Analysis of commercial humic acids*

183 First, two commercial humic acids WHA and AHA, which have been extensively used as
184 model humic acids by several researchers [13–15,27,28], were analyzed by Py-GC/MS. Fig. 2
185 shows the Py-GC/MS pyrogram of WHA and AHA, and Table 1 lists the detected compounds.
186 The major products obtained from the pyrolysis of coal-derived WHA were aromatic compounds
187 (n = 1, 3, 4, 5, 7, 8, 10, 13, 14, 17, 20, and 23) attributed to a high degree of humification; these
188 compounds were consistent with brown coal humic substances [29]. On the other hand, the major
189 products obtained from the pyrolysis of peat-derived AHA were a series of aliphatic compounds
190 (n = 2, 6, 8, 9, 11, 12, 15, 16, 18, 19, 21, 22, and 24–32), attributed to lipids and paraffinic
191 material in humic substances. The result obtained for AHA is similar to that obtained for
192 peat-derived humic substances [29,30]. The composition of organic colloids in deep groundwater
193 is similar to that of humic substances with high humification [12]. Thus, we used WHA as a
194 model organic colloid in the following experiments.

195

196 *3.2. Condensation of humic acid*

197 *3.2.1. Optimum hydrodynamic conditions*

198 The effects of the TMP and stirring rate on the condensation of WHA were investigated to
199 obtain optimum hydrodynamic conditions for the NF process. Fig. 3 shows the effect of the
200 hydrodynamic conditions on the permeate flux and WHA concentration in the condensed
201 solutions. In this figure, the theoretical concentrations in the condensed solutions with 100%
202 recovery yield are represented as dotted lines. The recovery yield was defined as the amount of

organic colloids in the condensed solution divided by that in the initial solution. Fig. 4 shows the surface view of the membranes after 5-fold condensation tests of WHA. The condensation test under all hydrodynamic conditions exhibited no reduction in flux (Fig. 3). However, all WHA concentrations in the condensed solutions were below the dotted line, indicating low recovery yields. As shown in Fig. 3a, the recovery yield after condensation at 150 rpm and 1.5 MPa was quite low, only 44% (Fig. 3a). This low recovery yield was caused by the adsorption and deposition of humic acid on the membrane surface. As shown in Fig. 4a, large amounts of humic acids were deposited on the membrane surface. The stirring rate on the membrane surface is considered greater outside the membrane cell compared with that in the center. Thus, a large amount of deposits on the center of the membrane surface is probably caused by the distribution of the stirring rate. However, at this time scale, these deposits hardly affected the reduction in flux. As the stirring rate increased or TMP decreased, the recovery yields increased (Figs. 3b and c), and the amounts of humic acids deposited on the membrane surface decreased (Figs. 4b and c). The decreasing TMP and increasing stirring rate decrease the permeation drag and concentration polarization of solutes on the membrane surface, resulting in the prevention of membrane fouling. At a high stirring rate and low TMP, a high recovery yield of 80% was obtained (Fig. 3d), with small amounts of WHA deposited on the NF membrane (Fig. 4d). These results indicate that a high stirring rate and low TMP is optimum condition for high recovery yield. Because the available value of the stirring rate in our apparatus was maximally limited to be 1500 rpm, and a significantly low TMP led to increased experiment time, the condensation test was conducted at a stirring rate of 1500 rpm and 0.75 MPa as the optimized condition. For comparison, condensation tests were carried out at a stirring rate of 150 rpm and 1.5 MPa. We also confirmed this optimization was effective in the case using the p(MPC-co-AEMA)-coated

NF membranes as described section 3.2.2 and 3.3.

3.2.2. Modification of membrane surface

To prevent the adsorption of organic colloids, the surface of the NF membrane was modified with zwitterionic polymer. Fig. 5 shows the effect of the p(MPC-co-AEMA) concentration on the ζ-potentials and water contact angles of the NF membranes. The ζ-potential of the NF membranes was neutralized by the coating with the aqueous solution of 0.0001 wt% p(MPC-co-AEMA). The water contact angle of the NF membranes decreased with increasing the p(MPC-co-AEMA) concentration and reached the minimum value at 0.01 wt% p(MPC-co-AEMA). Fig. 6 shows the effect of the p(MPC-co-AEMA) concentration on the recovery yields and experimental times required to condensate the feed solution to 5 times on the WHA condensation test. The highest recovery yield was obtained at 0.1 wt% p(MPC-co-AEMA). These results indicate the coating with the aqueous solution of 0.1 wt% p(MPC-co-AEMA) made the surface of the NF membranes more hydrophilic and prevented the adsorption of organic colloids more effectively. Thus, the NF membranes were coated with 0.1 wt% of p(MPC-co-AEMA) on the following experiments.

We examined the effect of the hydrodynamic conditions and membrane surface modification on the recovery yields of WHA. Fig. 7 shows the time courses of the permeate flux and WHA concentrations in the condensation tests using the p(MPC-co-AEMA)-coated NF membrane. Fig. 8 shows the surface view of the p(MPC-co-AEMA)-coated NF membrane after 5-fold condensation tests of WHA. As shown in Fig. 7, in the condensation test using the p(MPC-co-AEMA)-coated NF membrane (Fig. 7), reduction in flux was not observed. Although the amounts of humic acids deposited on the surface of the p(MPC-co-AEMA)-coated NF

membrane (Figs. 8a and b) and raw NF membrane (Figs. 4a and d) seemed similar, recovery yields of 56% and 86% for the p(MPC-co-AEMA)-coated NF membrane shown in Figs. 7a and b were higher than those of the raw NF membrane under the same hydrodynamic condition (44% and 80% shown in Figs. 3a and d, respectively). Thus, modification of the membrane surface with p(MPC-co-AEMA) is effective against fouling by WHA, caused by improved hydrophilicity. In addition, the optimized hydrodynamic condition was also effective to improve the recovery yields in the case using the p(MPC-co-AEMA)-coated NF membrane.

3.3. Condensation of BSA

We examined the effects of hydrodynamic conditions and membrane surface modification on the recovery yields of BSA. Fig. 9 shows the time courses of the permeate flux and BSA concentration in the condensed solutions. The initial permeate flux value of the raw NF membranes (Figs. 9a and b) was significantly lower than those obtained from the condensation test of WHA under the same hydrodynamic condition (Fig. 3a and d), indicating that the permeate flux of raw NF membranes drastically declines immediately after the start of the condensation test of BSA. On the other hand, the permeate flux in the condensation tests using the p(MPC-co-AEMA)-coated membranes (Fig. 9c and d) exhibited almost the same values as those obtained from the condensation test of WHA under the same hydrodynamic conditions (Fig. 7a and b). Thus, the modification of the membrane surface with p(MPC-co-AEMA) is significantly effective for the prevention of the decrease in permeate flux by fouling with BSA. The recovery yields were significantly improved by the optimized hydrodynamic conditions (Fig. 9b) as compared to the membrane surface modified with p(MPC-co-AEMA) (Fig. 9c), indicating that the optimized hydrodynamic conditions are more effective than the membrane surface

modified with p(MPC-co-AEMA) for increasing the recovery yield of BSA.

3.4. Condensation of organic colloids in groundwater

We examined the effects of hydrodynamic conditions and membrane surface modification on the recovery yield of organic colloids in groundwater. Fig. 10 shows the time course of the permeate flux and organic colloid concentration in the condensed solution. The condensation test using the raw NF membrane under the original hydrodynamic condition exhibited no reduction in flux, but the recovery yield at 5-fold condensation was only 62% (Fig. 10a). This low recovery yield is attributed to the adsorption of organic colloids on the membrane surface caused by membrane fouling. On the other hand, the condensation test using the p(MPC-co-AEMA)-coated NF membrane under the optimized hydrodynamic condition afforded a higher recovery yield of 92% at 5-fold condensation (Fig. 10b). For obtaining a sufficiently high concentration of organic colloids for Py-GC/MS measurement, the groundwater was condensed from 500 mL to 25 mL (20-fold condensation) using the p(MPC-co-AEMA)-coated NF membrane under the optimized hydrodynamic condition. Fig. 11 shows the results. The recovery yield obtained was 74% at 20-fold condensation, which was higher than that of 57% at 20-fold condensation in our previous study using the raw NF membrane under the original hydrodynamic condition (at 150 rpm and 1.5 MPa) [12]. Thus, we achieved improvement in the recovery yield of organic colloids by the combination of optimized hydrodynamic conditions and p(MPC-co-AEMA) coating. Groundwater generally contains inorganic colloids such as fragments of granites and clay minerals resulting from dissolution and precipitation of host rock [31]. Inorganic colloids would also cause membrane fouling during the condensation process, although the membrane fouling with inorganic colloids was not observed in this study. The optimization of hydrodynamic

conditions would also be promising for preventing fouling with inorganic colloids. Further evaluation about the effect of inorganic colloids on condensation of organic colloids is necessary.

3.5. Characterization of organic colloids in groundwater

Fig. 12 shows the Py-GC/MS pyrogram of the organic colloids in the condensed groundwater, and Table 1 lists the detected compounds. The major products obtained from the pyrolysis of organic colloids were aromatic products. This result indicates that the composition of a majority of the organic colloids in deep groundwater is similar to that of humic substances with high humification, as has been previously reported by our group [12]. Moreover, as shown in Fig. 12b, the major products obtained from the pyrolysis of p(MPC-co-AEMA), such as benzene, methyl methacrylate, and dimethylethanolamine, were not detected in the pyrogram of organic colloids, indicating that the p(MPC-co-AEMA) coating does not desorb from the NF membrane surface and does not affect Py-GC/MS analysis. Although the result obtained from the Py-GC/MS pyrogram was not different from those obtained from our previous study [12], other components, which were not detected by Py-GC/MS, may be different. In particular, the result of rare earth elements (REEs) could be different, caused by their high affinity with organic colloids [32–34]. REEs are regarded as analogs of trivalent actinides [35] and are important for HLW. Therefore, REEs should be analyzed in future studies.

4. Conclusions

We examined the improvement in the recovery yields of organic colloids via the condensation of deep groundwater by utilizing optimized hydrodynamic conditions, such as transmembrane applied pressure and stirring rate, and modifying the surface of NF membranes with

p(MPC-co-AEMA). The recovery yield of humic acid from the condensation test was increased by the optimized hydrodynamic conditions, attributed to the reduction of concentration polarization and permeate drag, and by the modification of membrane surfaces, attributed to the hydrophilization of the NF membrane surface. The recovery yield of BSA in the condensation test was also increased by the optimized hydrodynamic conditions and membrane surface modification. In addition, the modification of membrane surfaces was effective for preventing the decrease in permeate flux, caused by BSA fouling. The recovery yield of organic colloids in the condensation test of deep groundwater was significantly increased by the combination of optimized hydrodynamic conditions and the membrane surface modification. The Py-GC/MS analysis of organic colloids condensed by the improved method proposed in this study indicated that composition of organic colloids is similar to that of humic substance with high humification, same as in our previous study. The optimization of hydrodynamic conditions and modification of membrane surfaces, which were effective for the improvement in the recovery of organic colloids, will contribute to the prevention of organic fouling in various applications of NF membranes.

Acknowledgments

We would like to thank Prof. R. Takagi (Kobe Univ.) for his fruitful discussion and useful comments.

References

[1] Minister of Economy, Trade and Industry, Designated Radioactive Waste Final Disposal Act (Act No. 117 of 2000), 2000.

[2] P. Vilks, D.B. Bachinski, Characterization of organics in Whiteshell Research area groundwater and the implications for radionuclide transport, Appl. Geochem. 11 (1996) 387–402.

[3] T. Saito, Y. Suzuki, T. Mizuno, Size and elemental analyses of nano colloids in deep granitic groundwater: implications for transport of trace elements, Colloids Surf. A: Physicochem. Eng. Asp. 435 (2013) 48–55.

[4] V. Moulin, G. Ouzounian, Role of colloids and humic substances in the transport of radio-elements through the geosphere, Appl. Geochem. 7 (1992) 179–186.

[5] V. Moulin, C. Moulin, Fate of actinides in the presence of humic substances under conditions relevant to nuclear waste disposal, Appl. Geochem. 10 (1995) 573–580.

[6] J. Gaillardet, J. Viers, B. Dupré, Trace elements in river waters, in: J.I. Drever(Ed.), Treatise on Geochemistry, Elsevier, Amsterdam, (2003) 225–272.

[7] M. Plaschke, J. Romer, J.I. Kim, Characterization of Gorleben groundwater colloids by atomic force microscopy, Environ. Sci. Technol. 36 (2002) 4483–4488.

[8] E.M. Thurman, R.L. Malcom, Preparative isolation of aquatic humicsubstances, Environ. Sci. Technol. 15 (1981) 463–466.

[9] C.J. Miles, J.R. Tuschall Jr., P.L. Brezonik, Isolation of aquatic humus with diethylaminoethylcellulose, Anal. Chem. 55 (1983) 410–411.

[10] S.M. Serkiz, E.M. Perdue, Isolation of dissolved organic matter from the Suwannee River using reverse osmosis, Water Res. 24 (1990) 911–916.

[11] L. Sun, E.M. Perdue, J.F. McCarthy, Using reverse osmosis to obtain organic matter from surface and ground waters, Water Res. 29 (1995) 1471–1477.

[12] D. Aosai, D. Saeki, T. Iwatsuki, H. Matsuyama, Concentration and characterization of

organic colloids in deep granitic groundwater using nanofiltration membranes for evaluating radionuclide transport, Colloids and Surf. A: Physicochem. Eng. Asp. 485 (2015) 55–62.

[13] S. Hong, M. Elimelech, Chemical and physical aspects of natural organic matter (NOM) fouling of nanofiltration membranes, J. Membr. Sci. 132 (1997) 159–181.

[14] A. Seidel, M. Elimelech, Coupling between chemical and physical interactions in natural organic matter (NOM) fouling of nanofiltration membranes: implications for fouling control, J. Membr. Sci. 203 (2002) 245–255.

[15] C.Y. Tang, Y.N. Kwon, J.O. Leckie, Fouling of reverse osmosis and nanofiltration membranes by humic acid—effects of solution composition and hydrodynamic conditions, J. Membr. Sci. 290 (2007) 86–94.

[16] M.J. Avena, L.K. Koopal, W.H. van Riemsdijk, Proton binding to humic acids: Electrostatic and intrinsic interactions. J. Colloid Interface Sci. 217 (1999) 37–48.

[17] C.L. Tiller, C.R. Omelia, Natural organic matter and colloidal stability: Models and measurements, Colloids and Surf. A: Physicochem. Eng. Asp. 73 (1993) 89–102.

[18] K. Ghosh, M. Schnitzer, Macromolecular structures of humic substances, Soil Sci. 129 (1980) 266–276.

[19] F.J. Stevenson, Humus chemistry, John Wiley & Sons: New York, 1982.

[20] D. Rana, T. Matsuura, Surface modifications for antifouling membranes, Chem. Rev. 110 (2010) 2448–2471.

[21] G.D. Kang, M. Liu, B. Lin, Y.M. Cao, Q. Yuan, A novel method of surface modification on thin-film composite reverse osmosis membrane by grafting poly(ethylene glycol), Polymer 48 (2007) 1165–1170.

[22] G.D. Kang, H.J. Yu, Z.N. Liu, Y.M. Cao, Surface modification of a commercial thin film

composite polyamide reverse osmosis membrane by carbodiimide-induced grafting with poly(ethylene glycol) derivatives, Desalination 275 (2011) 252–259.

[23] R. Bernstein, S. Belfer, V. Freger, Bacterial attachment to RO membrane ssurface-modified by concentration–polarization–enhanced graft polymerization, Environ. Sci. Technol. 45 (2011) 5973–5980.

[24] F. Razi, I. Sawada, Y. Ohmukai, T. Maruyama, H. Matsuyama, The improvement of antibiofouling efficiency of polyethersulfone membrane by functionalization with zwitterionic monomers, J. Membr. Sci. 401 (2012) 292–299.

[25] D. Saeki, T. Tanimoto, H. Matsuyama, Prevention of bacterial adhesion on polyamide reverse osmosis membranes via electrostatic interactions using a cationic phosphorylcholine polymer coating, Colloids and Surf. A: Physicochem. Eng. Asp. 443 (2014) 171–176.

[26] T. Ikuma, K. Takeuchi, K. Sagisaka, T. Takasawa, Coomassie brilliant blue G250 dye-binding microassay for protein, Obihiro University Archives of Knowledge 23 (2002) 18–26

[27] Y. Muramatsu, S. Uchida, P. Sriyotha, K. Sriyotha, Some considerations on the sorption and desorption phenomena of iodide and iodate on soil, Water, Air, Soil Pollut. 49 (1990) 125–138.

[28] M. E. Alcántara-Garduño, T. Okuda, W. Nishijima, M. Okada, Ozonation of trichloroethylene in acetic acid solution with soluble and solid humic acid. J. Hazard Mater. 160 (2008) 662–667.

[29] X.Q. Lu, J.V. Hanna, W.D. Johnson, Source indicators of humic substances: an elemental composition, solid state 13 C CP/MAS NMR and Py-GC/MS study, Appl. Geochem. 15 (2000) 1019–1033.

[30] F.J. Gonzalez-Vila, J. del Rio, G. Almendros, F. Martin, Structural relationship between humic fractions from peat and lignites from the Miocene Granada basin, Fuel 73 (1994) 215–221.

[31] D. Aosai, Y. Yamamoto, T. Mizuno, T. Ishigami, H. Matsuyama, Size and composition analyses of colloids in deep granitic groundwater using microfiltration/ultrafiltration while maintaining in situ hydrochemical conditions, Colloids and Surf. A: Physicochem. Eng. Asp. 461 (2014) 279–286.

[32] J.W. Tang, K.H. Johannesson, Speciation of rare earth elements in natural terres-trial waters: assessing the role of dissolved organic matter from the modeling approach, Geochim. Cosmochim. Acta 67 (2003) 2321–2339.

[33] Y. Yamamoto, Y. Takahashi, H. Shimizu, Systematic change in relative stabilities of REE–humic complexes at various metal loading levels, Geochem. J. 44 (2010) 39–63.

[34] F.J. Millero, Stability constants for the formation of rare earth–inorganic com-plexes as a function of ionic strength, Geochim. Cosmochim. Acta 56 (1992) 3123–3132.

[35] N. Chapman, J. Smellie, Introduction and summary of the workshop, Chem.Geol. 55 (3–4) (1986) 167–173.

Table 1 Typical compounds obtained from the pyrolysis of Wako humic acid (WHA), Aldrich humic acid (AHA), and organic colloids in groundwater condensed using the p(MPC-co-AEMA)-coated NF membrane under optimized hydrodynamic conditions (at 1500 rpm and 0.75 MPa).

Peak No.	Compound	Group
1	Toluene	Aromatic
2	Octene	Aliphatic carbon
3	Ethylbenzene	Aromatic
4	Xylene	Aromatic
5	Styrene	Aromatic
6	Nonene	Aliphatic carbon
7	Phenol and Benzonitrile	Hydroxy benzene and N-containing
8	Decene and C_3-Alkylbenzene	Aliphatic carbon and aromatic
9	Undecene	Aliphatic carbon
10	Naphthalene	Aromatic
11	Dodecene	Aliphatic carbon
12	Tridecene	Aliphatic carbon
13	Methylnaphthalene	Aromatic
14	Biphenyl	Aromatic
15	Tetradecene	Aliphatic carbon
16	Pentadecene	Aliphatic carbon
17	Fluorene	Aromatic
18	Hexadecene	Aliphatic carbon
19	Heptadecene	Aliphatic carbon
20	Phenanthrene	Aromatic
21	Octadecene	Aliphatic carbon
22	Nonadecene	Aliphatic carbon
23	Methylphenanthrene and Methylanthracene	Aromatic
24	Eicosene	Aliphatic carbon
25	Heneicosene	Aliphatic carbon
26	Docosene	Aliphatic carbon
27	Tricosene	Aliphatic carbon
28	Tetracosene	Aliphatic carbon
29	Pentacosene	Aliphatic carbon
30	Hexacosene	Aliphatic carbon
31	Heptacosene	Aliphatic carbon
32	Octacosene	Aliphatic carbon

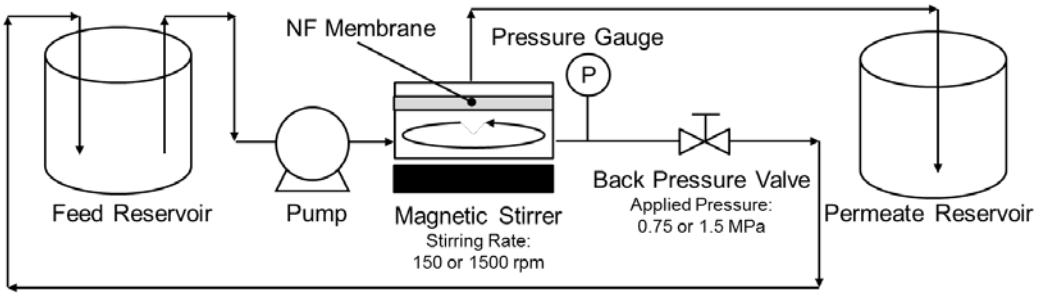

Fig. 1. Schematic of the cross-flow condensation apparatus.

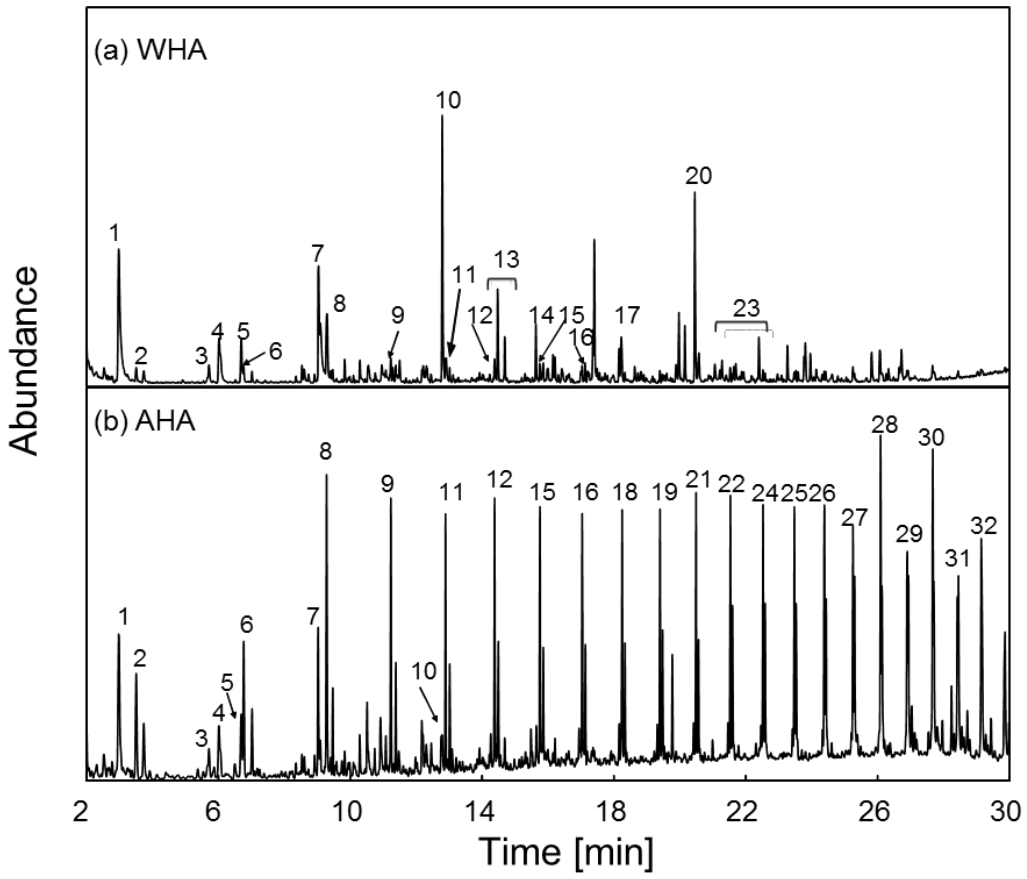

Fig. 2. Py-GC/MS pyrograms of (a) WHA and (b) AHA. Table 1 shows the peak numbers.

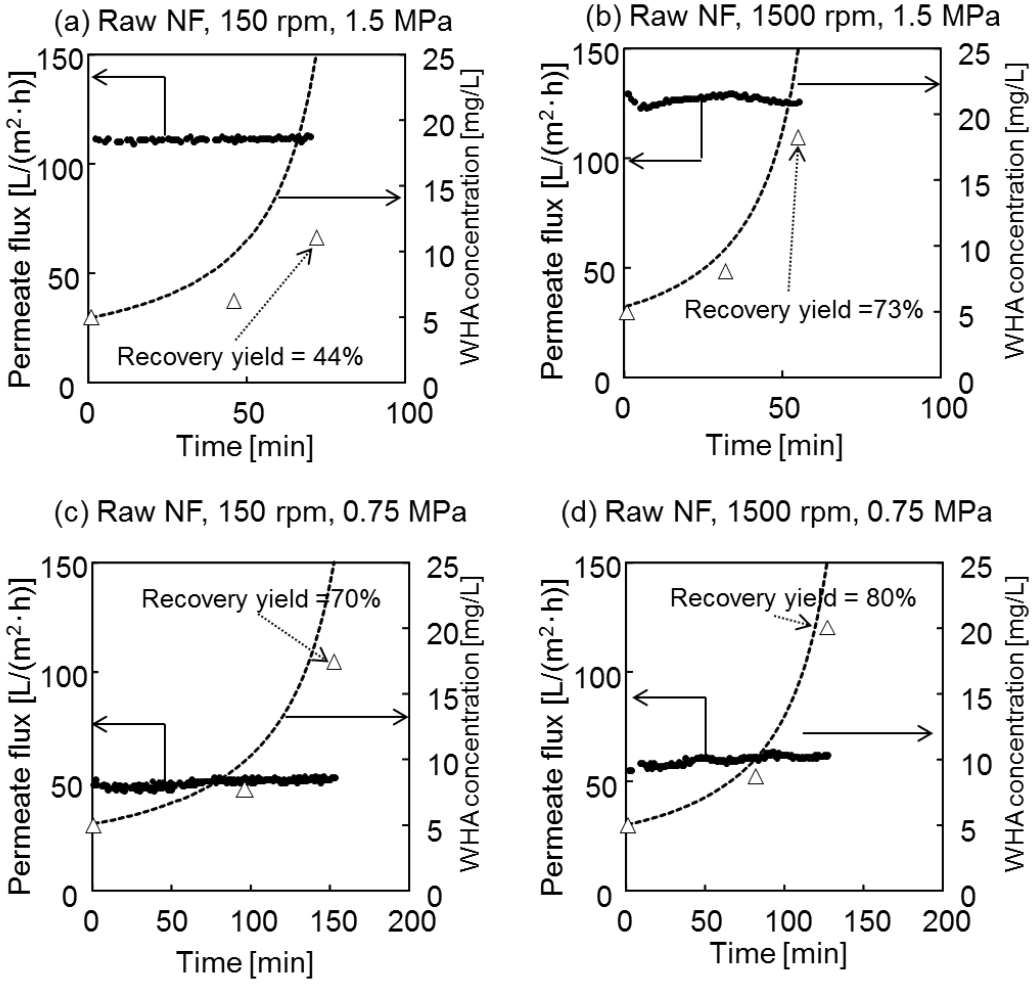

Fig. 3. Time courses of the permeate flux and WHA concentrations in the condensed solutions from the condensation tests of WHA using (a) raw NF membrane under the original hydrodynamic conditions (at 150 rpm and 1.5 MPa), (b) raw NF membrane at 1500 rpm and 1.5 MPa, (c) raw NF membrane at 150 rpm and 0.75 MPa, (d) raw NF membrane under the optimized hydrodynamic conditions (at 1500 rpm and 0.75 MPa). Closed circles and open triangles indicate permeate flux and WHA concentration, respectively. Dotted line indicates the theoretical concentrations of WHA assuming 100% recovery yield.

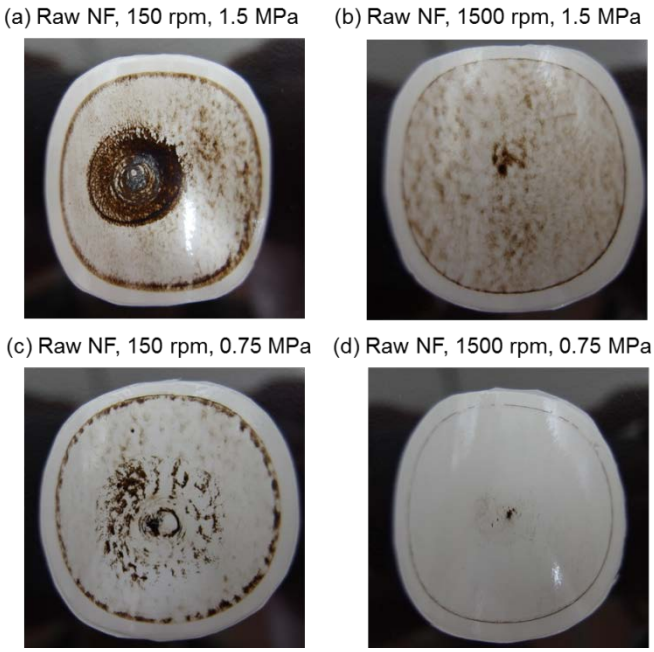

Fig. 4. Surface views of the membranes after the 5-fold condensation tests of WHA using (a) raw NF membrane under the original hydrodynamic condition (at 150 rpm and 1.5 MPa), (b) raw NF membrane at 1500 rpm and 1.5 MPa, (c) raw NF membrane at 150 rpm and 0.75 MPa, (d) raw NF membrane under the optimized hydrodynamic conditions (at 1500 rpm and 0.75 MPa).

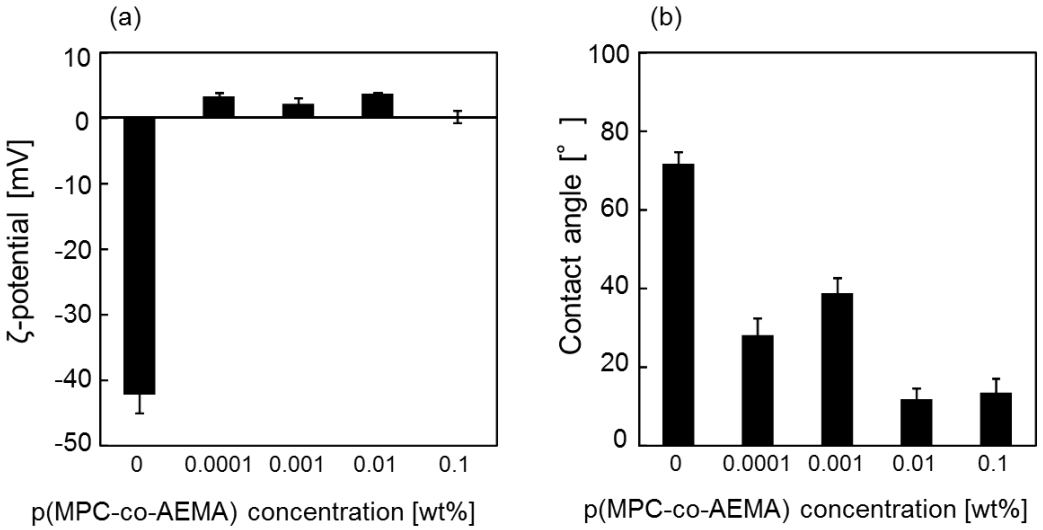

Fig. 5. ζ-potentials (a) and water contact angles (b) of the raw NF membrane and coated NF membranes with different concentrations of p(MPC-co-AEMA).

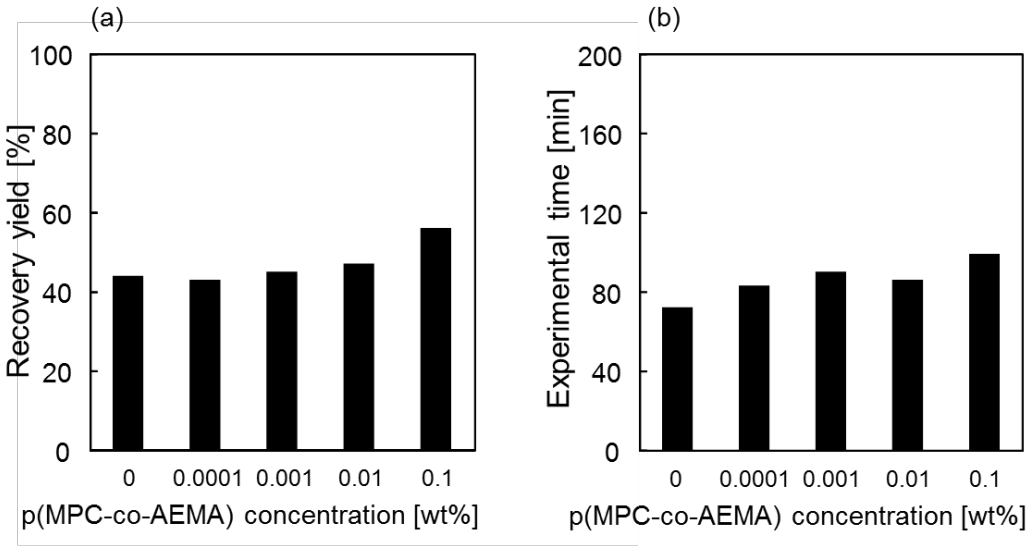

Fig. 6. Recovery yields (a) and experimental times (b) of the 5-fold concentration test of the humic acid at 1.5 MPa and 150 rpm using the raw NF membrane and coated NF membranes with different concentrations of p(MPC-co-AEMA).

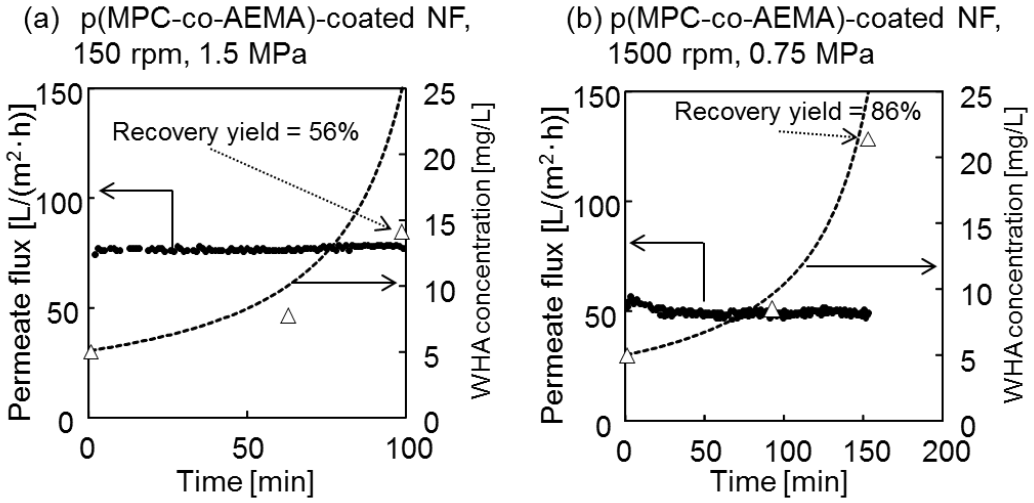

Fig. 7. Time courses of the permeate flux and WHA concentrations in the condensed solutions from the condensation tests of WHA using (a) p(MPC-co-AEMA)-coated NF membrane under the original hydrodynamic conditions (at 150 rpm and 1.5 MPa), (b) p(MPC-co-AEMA)-coated NF membrane under the optimized hydrodynamic conditions (at 1500 rpm and 0.75 MPa). Closed circles and open triangles indicate permeate flux and WHA concentration, respectively. Dotted line indicates the theoretical concentrations of WHA assuming 100% recovery yield.

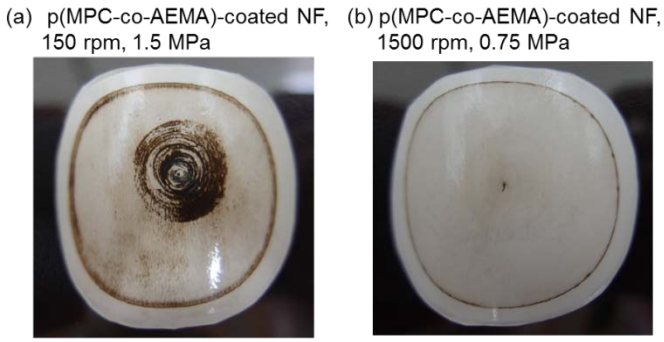

Fig. 8. Surface views of the membranes after the 5-fold condensation tests of WHA using (a) p(MPC-co-AEMA)-coated NF membrane under the original hydrodynamic condition (at 150 rpm and 1.5 MPa), (b) p(MPC-co-AEMA)-coated NF membrane under optimized hydrodynamic conditions (at 1500 rpm and 0.75 MPa).

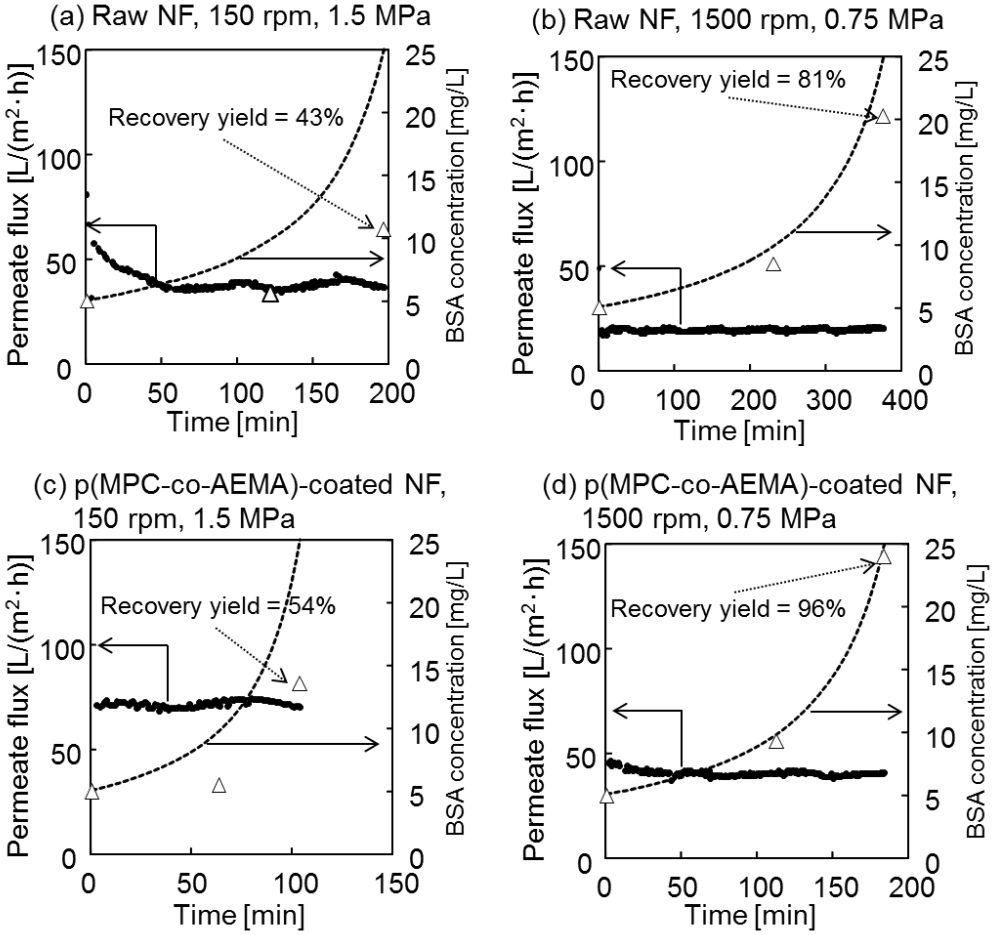

Fig. 9. Time courses of the permeate flux and BSA concentrations in the condensed solutions from the condensation tests of the BSA using (a) raw NF membrane under the original hydrodynamic condition (at 150 rpm and 1.5 MPa), (b) raw NF membrane under the optimized hydrodynamic conditions (at 1500 rpm and 0.75 MPa), (c) p(MPC-co-AEMA)-coated NF membrane under the original hydrodynamic condition (at 150 rpm and 1.5 MPa), (d) p(MPC-co-AEMA)-coated NF membrane under the optimized hydrodynamic conditions (at 1500 rpm and 0.75 MPa). Closed circles and open triangles indicate permeate flux and BSA concentration, respectively. Dotted line indicates the theoretical concentrations of BSA assuming 100% recovery yield.

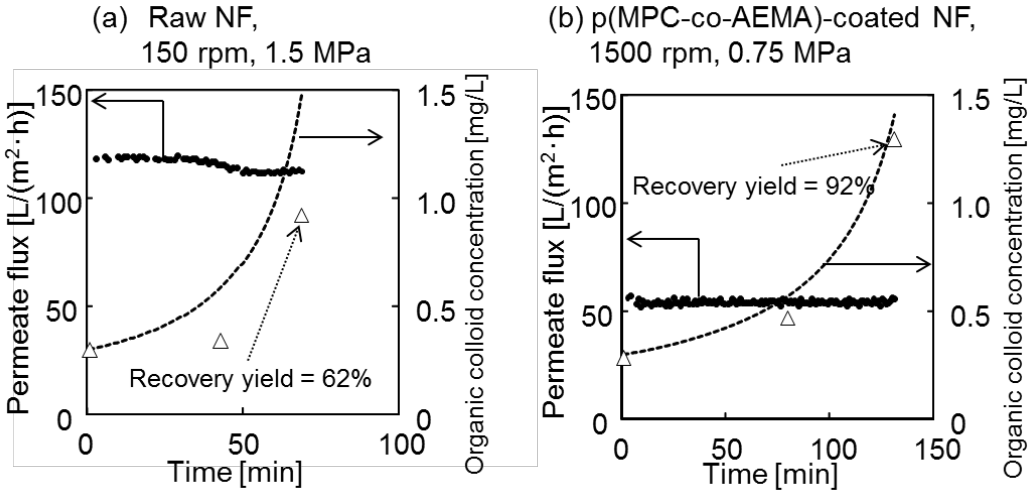

Fig. 10. Time courses of the permeate flux and organic colloid concentration of the condensed solutions from the condensation test of the groundwater using (a) raw NF membrane under the original hydrodynamic condition (at 150 rpm and 1.5 MPa), (b) p(MPC-co-AEMA)-coated NF membrane under the optimized hydrodynamic conditions (at 1500 rpm and 0.75 MPa). The concentration of organic colloids was calculated under the assumption that all organic colloids were WHA. Closed circles and open triangles indicate permeate flux and organic colloid concentration, respectively. Dotted line indicates theoretical concentrations of organic colloids assuming 100% recovery yield.

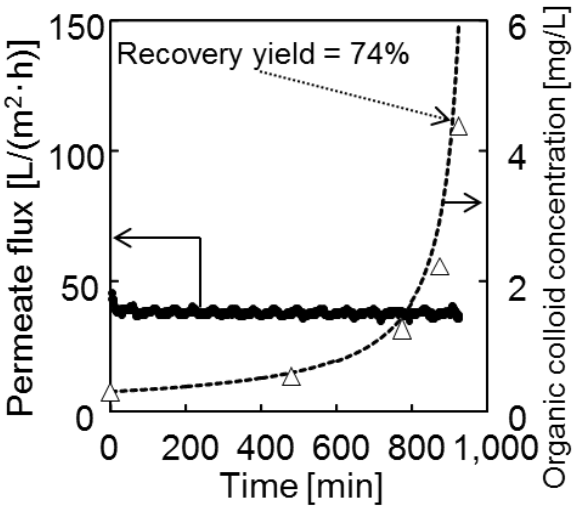

Fig. 11. Time courses of the permeate flux and organic colloid concentration in the condensed solutions from the condensation tests of the groundwater using the p(MPC-co-AEMA)-coated NF membrane under optimized hydrodynamic conditions (at 1500 rpm and 0.75 MPa). The groundwater was condensed from 500 mL to 25 mL. The concentration of organic colloids was calculated under the assumption that all organic colloids were WHA. Closed circles and open triangles indicate permeate flux and organic colloid concentration, respectively. Dotted line indicates theoretical concentrations of organic colloids assuming 100% recovery yield.

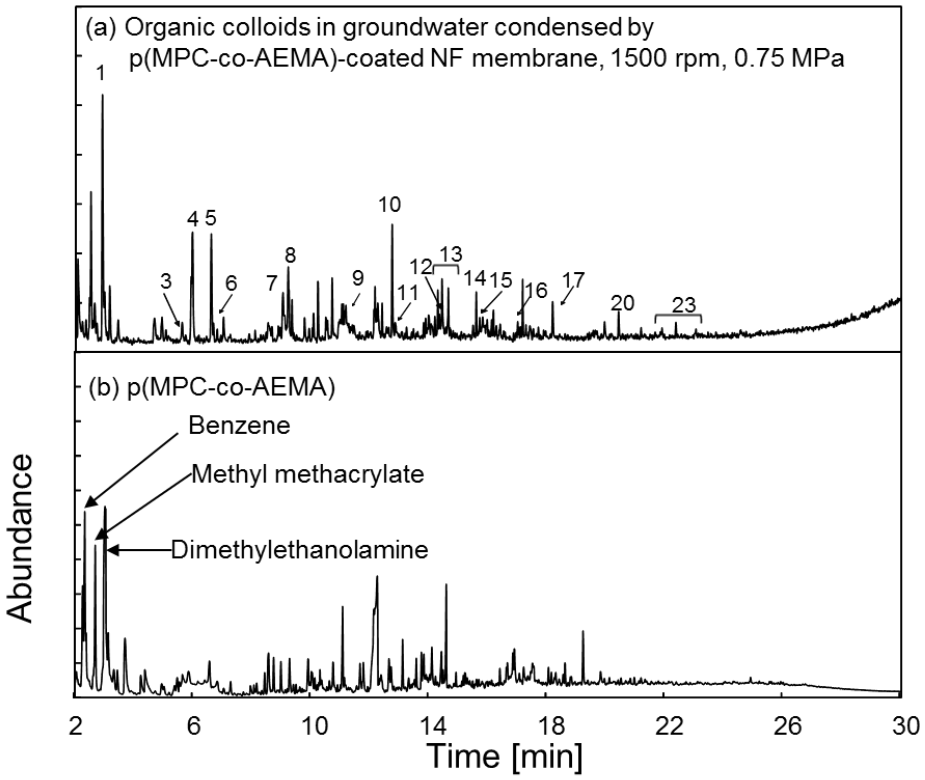

Fig. 12. Py-GC/MS pyrograms of (a) organic colloids in groundwater condensed by the p(MPC-co-AEMA)-coated NF membrane under optimized hydrodynamic conditions (at 1500 rpm and 0.75 MPa), (b) p(MPC-co-AEMA). Table 1 shows the peak numbers.